Article

Visible-Light Mediated Photocatalytic Aerobic Dehydrogenation of N-Heterocycles by Surface Grafted TiO2 and 4-Amino-TEMPO

Narmina O. Balayeva, Nan Zheng, Ralf Dillert, and Detlef W. Bahnemann

ACS Catal., **Just Accepted Manuscript** • DOI: 10.1021/acscatal.9b03322 • Publication Date (Web): 15 Oct 2019

Visible-Light Mediated Photocatalytic Aerobic Dehydrogenation of *N*-Heterocycles by Surface Grafted TiO_2 and 4-amino-TEMPO

Narmina O. Balayeva [a], Nan Zheng [b*], Ralf Dillert [a,c], Detlef W. Bahnemann [a,c,d*]*

[a] Institute of Technical Chemistry, Gottfried Wilhelm Leibniz University of Hannover, Callinstr. 5, D-30167 Hannover, Germany

[b] Department of Chemistry and Biochemistry, University of Arkansas, Fayetteville, AR 72701 (USA)

[c] Laboratory of Nano and Quantum Engineering, Gottfried Wilhelm Leibniz University of Hannover, Schneiderberg 39, D 30167 Hannover, Germany

[d] Laboratory "Photoactive Nanocomposite Materials", Saint-Petersburg State University, Ulyanovskaya str. 1, Peterhof, 198504 Saint-Petersburg, Russia

ABSTRACT:

Herein, the visible-light-induced dehydrogenation of N-heterocycles such as tetrahydroquinolines, tetrahydroisoquinolines, and indolines in O_2-containing suspensions of a commercially available titanium dioxide photocatalyst yielding the corresponding heteroarenes is presented. 4-amino-2,2,6,6-tetramethylpipiridinyloxyl (4-amino-TEMPO) was found to exhibit a beneficial role as it increased the yield and improved the selectivity of the dehydrogenation reaction. Both the selectivity and the yield are further enhanced by grafting 0.1 wt% Ni(II) ions onto the TiO_2 surface. It is proposed that the basic reactant adsorbs at Lewis acid sites present at the TiO_2 surface. The dehydrogenation reaction is initiated by visible light excitation of the resulting surface complex and a subsequent single electron transfer from the excited N-heterocycle via the conduction band of TiO_2 to O_2. Ni(II) ions possibly serve as an electron transfer bridge between the conduction band of TiO_2 and O_2, while the TEMPO derivative is assumed to act as a selective redox mediator involved in reactions of the generated reactive oxygen species.

KEYWORDS: dehydrogenation, N-heterocyclic amines, surface complex, TiO_2, visible light

INTRODUCTION:

N-heteroarenes are considered as a privileged structure in medicinal chemistry and material science enabling requisite functionalities. Therefore, the development of innovative methods for *N*-heteroarene synthesis as well as for the improvement of existing synthesis methods became an essential topic in contemporary organic synthesis.[1,2] Compared to the commonly used cross-coupling strategy that relies on the availability of the pre-functionalized heteroarene precursors,

dehydrogenation of *N*-heterocycles provides a complementary approach capable of introducing substituents to the saturated *N*-heterocycle core. This feature overcomes constraints of the precursor in the former approach and thus permits the synthesis of substituted *N*-heteroarenes that are not accessible by the cross-coupling reaction.

In general, the dehydrogenation of N-heterocyclic amines is classified into two subclasses: acceptorless and acceptor assisted dehydrogenation, depending on whether a hydrogen atom acceptor is used. Organometallic complexes composed of Ru, Ni, Co, or Ir have been extensively developed as homogenous catalysts for the acceptorless dehydrogenation of *N*-heterocycles, [3–7] however, the catalysts in these reaction systems are not recyclable. Therefore, alternative carbon-supported metal catalysts[8] such as hydroxyapatite-bound Pd [9] and Pt/C [10] have been used to replace the organometallic complexes in the acceptorless dehydrogenation. Most recently, Pd-doped hydrotalcite catalysts were used for the acceptorless dehydrogenation of both, primary and secondary amines at 140°C in the p-xylene solvent.[11] Similarly, an acceptorless dehydrogenative aromatization of cyclic amines by Pd/LDH (layered double hydroxide) catalysts was also reported.[12] Nevertheless, most of the existing heterogeneous catalytic systems employed for the acceptorless dehydrogenation involve noble metals or require relatively forcing reaction conditions (e.g., temperatures >140 °C and/or long reaction times) thus restricting their applicability on large scales.

On the other hand, for the acceptor assisted dehydrogenation, various chemical oxidants such as 2,3-dichloro-5,6-dicyano-l,4-benzoquinone[13], chloranil[14], and selenium [8] have been used in stoichiometric amounts as the respective hydrogen acceptor. Conversely to these harsh methods, considerable endeavors have been laid on the oxidative dehydrogenation of N-heterocycles based on homogeneous catalysts such as copper [15,16] or oxyvanadium-based systems[17] in air or O_2

environment. The heterogeneous counterpart has also been studied noticeably, with quite diverse catalysts such as transition metal or metal oxide nanoparticles on graphene or activated carbon, [18–21] gold nanoclusters[22], etc. having been reported to promote the dehydrogenation reactions.

Unlike the approaches mentioned above, visible-light-harvesting photocatalytic dehydrogenation reactions can be successfully performed under considerable milder reaction conditions. Nevertheless, the true potential of photo-induced dehydrogenation catalysis is still rather unexplored compared to the metal-catalyzed thermal dehydrogenation processes. For example, the visible light-mediated oxidative dehydrogenation of *N*-heterocycles at ambient temperature using $Ru(bpy)_3Cl_2 \cdot 6H_2O$ [23] and a dual catalyst system employing the Fukuzumi acridinium salt with $Pd(BF_4)_2$ as photocatalysts have recently been reported.[24] Later, rose Bengal has been used to replace organometallic complexes for the dehydrogenation of N-heteroarenes.[25] The dehydrogenation of *N*-heterocycles under oxygen free inert condition and at room temperature was also studied employing $Ru(bpy)_3Cl_2 \cdot 6H_2O$ as visible-light active photosensitizer coupled with $Co(dmgH)_2PyCl$ as co-catalyst.[26] Regardless of the improved reaction conditions, the recyclability and the cost-efficiency are still remaining as main issues because of the employed organometallic complexes.

Therefore, herein a visible light-mediated dehydrogenation method for *N*-heterocycles using a heterogeneous recyclable and economical photocatalyst is presented for the first time **(Scheme 1.)**. For this purpose, TiO_2 was used as the main photocatalyst. TiO_2 is one of the most active and also widely used heterogeneous photocatalysts due to some outstanding features such as stability, non-toxicity, as well as cost-efficiency, abundancy, and reusability. Furthermore, photocatalytically active TiO_2 is commercially available in both, high quality and sufficient quantity. Although TiO_2 has been extensively exploited as photocatalyst for energy and

environmental applications, its use in organic synthesis remains rather unexplored particularly compared to homogeneous photocatalysts such as ruthenium and iridium complexes or organic dyes.[27] On the other hand, due to its large bandgap energy ($Eg_{(rutile)}$=3.0 eV, $Eg_{(anatase)}$=3.2 eV), titania can only be excited by UV light, which usually results in poor chemoselectivity. To address the intrinsic limitations of TiO_2 and develop a visible-light active photocatalytic system, numerous new strategies have been considered and employed. [28,29] It was found that upon adsorption of tertiary amines on the surface of TiO_2, a visible-light-harvesting surface complex is formed due to Lewis acid-base interactions resulting in a red-shift of the absorption spectrum by about 10 nm. [30–33] Such approach avoids the formation of holes in the valence band of the semiconductor that often provoke overoxidation in TiO_2-catalyzed photochemistry. Thus, instead of excitation of an electron from the valence band to the conduction band in TiO_2, the adsorbed amine injects an electron to the conduction band, which in turn donates this electron to O_2, yielding the superoxide radical anion. Previously, a similar approach has also been utilized to develop a Diels–Alder reaction of indoles with electron-rich dienes in which indole-TiO_2 surface complexes are formed and identified as being responsible for visible light absorption.[34,35] Moreover, the visible-light mediated oxidation of primary and secondary amines into the corresponding imines employing surface complexes of different organic molecules such as phenol[36], catechol[37], *N*-hydroxyphthalimide[38], and salicylic acid[39] on TiO_2 in the presence of TEMPO derivatives has been reported.

In the present work, transition metal nanoparticles or ions have been grafted onto the TiO_2 surface to further improve the photocatalytic activity of TiO_2 for the dehydrogenation of N-heterocycles. Most likely these grafted metal ions on the surface of the TiO_2 photocatalyst serve as electron shuttles thus transferring the excited electrons to O_2 and hence retarding their fast

decay.[40] Additionally, cooperative catalysts have been designed merging the TiO_2 photocatalyst with different derivatives of TEMPO to improve the overall chemoselectivity of the system. We thus developed a selective photocatalytic aerobic dehydrogenation method for N-heterocycles (tetrahydroquinolines, tetrahydroisoquinolines, indolines, and others) by employing surface grafted, commercially available UV-100 (TiO_2) photocatalyst and 4-amino-TEMPO upon visible light illumination.

It was found that Lewis acid surface sides on TiO_2 enable the surface complexation between the base sides of N-heterocycles acting as photosensitizers which are excited by visible light to initiate a single electron transfer from the N-heterocycle via the conduction band of TiO_2 to O_2. The resulting superoxide radical is likely involved in the dehydrogenation of the amine radical cation to yield the N-heteroarenes. The critical role of 4-amino-TEMPO for improving the selectivity and the reaction yield over 90% by creating an oxidizing surface saturated with H_2O_2 (byproduct) is discussed. Both, the selectivity and the reaction yield are further enhanced by grafting 0.1 wt% Ni(II) ion onto TiO_2 in which the nickel ions serve as electron transfer bridges between the conduction band of TiO_2 and adsorbed molecular oxygen. A plausible reaction mechanism is proposed and discussed.

EXPERIMENTAL SECTION

Synthesis of the photocatalysts:

Commercial TiO_2 (Hombikat UV-100 from Venator with 100% anatase crystal phase and ~ 320 m^2/g specific surface area) has been used as the photocatalyst (materials section is presented in the Supporting Information, SI). The grafting of Fe(III), Cu(II), Ni(II), Co(II), or Nb(V) nanoclusters on the surface of UV-100 was performed by following a simple impregnation method that has been reported before. [28,40,41] In brief, metal salts with the appropriate ratio (0.1

wt %) relative to titania were added into an aqueous TiO_2 suspension and stirred at 90 °C for 1 h to attain metal ion nanoclusters on the surface of TiO_2. Subsequently, the suspension was rinsed and centrifuged 3 times with copious amounts of deionized water. Afterward the precipitate was dried at 110 °C for 24 h and milled into a fine powder. To prepare 0.1 wt % Pt, Rh, and Pd photo-deposited TiO_2 photocatalysts, a 50 mL single neck reactor was taken. The appropriate amount of metal precursor salt was dissolved into 20 mL of methanol/deionized water mixture (1:3 ratio), and 1 g of commercial TiO_2 UV-100 was added into the system before closing the reactor. The suspension was continuously stirred for 24 h under 1 mW/cm^2 UV light irradiation. Afterward, the suspension was centrifuged, and the powder was rinsed three times with 50 mL of water. The obtained precipitant was dried at 110 °C for 24 h.

To gain some insight into the structure of the as-prepared surface grafted TiO_2 (namely Ni(II)/TiO_2), we used a series of characterization techniques including X-ray diffraction (XRD) (SI Figure S2), transmission electron microscopy (TEM) (SI Figure S3), diffuse reflectance spectroscopy (DRS) (SI Figure S4), FTIR spectroscopy, Brunauer–Emmett–Teller (BET), N_2 adsorption-desorption isotherms (SI Figure S8), and electron-paramagnetic resonance spectroscopy (EPR) (SI Figure S9). The content of Ni ions grafted onto TiO_2 surface was determined using ICP-OES measurement. Instrumental conditions and detailed characterization techniques are presented in the SI.

Photocatalytic Reaction Procedure:

10 mg TiO_2 or surface-modified TiO_2 (0.03 mol·L^{-1}) dispersed in 4 mL of an appropriate solvent were filled in an oven dried 20 mL vial employed as the photoreactor. 4-amino-TEMPO or different TEMPO derivatives (13.7 mg, 0.08 mmol, 20 mol% respective to the substrate) and 1, 2, 3, 4-tetrahydroquinoline (0.4 mmol) or other substrates were added to the suspension. The

reaction mixture was sonicated for 5 min until the TiO_2 catalyst was completely dispersed. After tightly sealing the suspension, the reaction environment was purged with molecular oxygen for about 20 min to displace any air present in the reactor. The reaction was carried out for 24 h under visible light illumination (LED array with λ_{max}=453 nm) with continuous stirring. Afterward, the catalyst was separated from the reaction mixture by centrifuging. The product was isolated employing flash column chromatography. In the case of optimization reactions, shown in **Table 1**, benzyl alcohol (20.6 μL, 0.2 mmol, 50 mol %) was added to the solution as an internal standard. 1, 2, 3, 4-Tetrahydroquinoline was chosen as the representative substrate to optimize the reaction conditions.

The corresponding calibration curves of the starting material (reactant) and the product were obtained by GC-FID (gas chromatography - flame ionized detector). The yield and the rest of the reactant were calculated with the calibration curves equation obtained by GC-FID. (For details see Fig. S1(a) and S1(b) in the SI). In brief, the yield of the product (Y), the conversion of the reactant (C), and the selectivity of the reaction (S) have been calculated employing the equations

$$Y = \frac{n_p}{n_{R_0}} \times 100 \quad (1)$$

$$C = \frac{n_{R_0} - n_R}{n_{R_0}} \times 100 \quad (2)$$

$$S = \frac{Y}{C} \times 100 \quad (3)$$

where n_p is the amount of the product, $n_{R_0}$is the starting amount of the reactant, and n_R is the remaining amount of the reactant.

The apparent quantum yield (Φ_{app}) of product formation has been calculated to compare the photocatalytic activity of the established reaction conditions (**Table 1**). The apparent quantum yield (Φ_{app}) was calculated with Φ_{app} = rate of formation / photon flux.

The photon flux was calculated with

$$photon\ flux = \frac{I \cdot A \cdot \lambda}{N_A \cdot h \cdot c} \quad (4)$$

and the irradiance $I = 4$ mW/cm^2, the irradiated area A= 4 cm^2, and the wavelength λ=453 nm. N_A, h, and c are the Avogadro constant, Planck number, and speed of light, respectively.

RESULTS AND DISCUSSION:

The absorption spectra of UV-100, UV-100 with 1,2,3,4-tetrahydroquinoline (1,2,3,4-THQ) in CH_3CN solvent has been measured to scrutinize the effect of N-heterocyclic amines on the absorption spectrum of TiO_2 and to determine the suitable wavelength of light source for the dehydrogenation reactions **(Figure 1)**. A solution of 1,2,3,4-THQ in CH_3CN absorbs at wavelengths lower than 350 nm while TiO_2 in CH_3CN absorbs at wavelengths lower than 380 nm. However, a significant red-shift about 60 nm is observed in the absorption spectra of TiO_2 suspensions containing 1,2,3,4-THQ which is clear evidence for the formation of a visible light-responsive surface-complex. In comparison, no red-shift is observed in the presence of non-semiconducting SiO_2 with a high surface area, and the absorption edge observed at about 350 nm and weak absorption edge up to 450 nm corresponds to 1,2,3,4-tetrahydoquinoline. These results strongly suggested that the surface complex is formed due to the Lewis acid (TiO_2)/base (tetrahydroquinolines) interaction. To support this data, an ATR-FTIR spectroscopy measurement was performed, and the band at around 1600 cm^{-1} and 3400 cm^{-1} corresponding to a free amine group vanished upon the addition of TiO_2 (UV-100). This ATR-FTIR data was another clear evidence of the surface-complex formation (**Figure 2**).

Inspiring from this evidence, we conducted the optimization reactions using 1,2,3,4-THQ as the model substrate, under blue light illumination (λ=453 nm) over UV-100 and 1 atm O_2 in CH_3CN (Table 1, entry 1) for 24 h. The completely dehydrogenated quinoline was formed with a yield of 35%. However, the selectivity was found to be rather poor. Addition of 4-amino-TEMPO (Table 1, entry 2) or TEMPO (Table 1, entry 3) almost doubled the selectivity, yielding quinoline in 79% yield. While, TEMPO was found to be stable during illumination, 4-amino-TEMPO was degrading gradually and after 24 h of illumination no peak associated to 4-amino-TEMPO was observed in the GC-FID chromatogram. Control studies showed that both, the photocatalyst UV-100 (Table 1, entry 5) and light (Table 1, entry 6) was essential for the dehydrogenation. O_2 was found to be also critical for the reaction as no reaction occurred in an inert (argon) atmosphere with UV-100 or Ni/UV-100 as the photocatalyst (see SI Table S1, entry 5 and 6). A LED lamp emitting at a wavelength of 453 nm was found to be optimal light source. Employing a 505 nm LED lamp resulted in a significant decrease of the reaction yield (see SI Table S1, entry 7 and 8). Replacement of UV-100 by P25 (commercial TiO_2 from Evonik Degussa, with ~50 m^2/g surface area, 20% rutile and 80% anatase) significantly reduced the yield and the conversion (Table 1, entry 4). On the other hand, control reactions with different metal oxides such as Al_2O_3, WO_3, ZnO, and SiO_2 gave negligible yields (See SI Table S2, entries 1-4). This is in agreement with the absorption spectroscopy results of 1,2,3,4-THQ and SiO_2 mixture evincing that this oxide is not capable of catalyzing the dehydrogenation reaction due to non-occurring surface complexation (SI, Table S2. entry 4). Solvent studies revealed that CH_3CN and *i*-PrOH are suitable dispersants, where *i*-PrOH shows slightly better activity for the visible light-mediated dehydrogenation of tetrahydroquinoline in the presence of a heterogeneous photocatalyst (SI Table S1, entries 1-4). To further improve the selectivity and

the yield, we investigated various metal ions grafted and noble metal photodeposited UV-100 as the photocatalyst. Metal ion grafted UV-100 (Cu^{2+}, Ni^{2+}, Co^{2+}, Fe^{3+}, Nb^{5+}) consistently show improved selectivity and yield in comparison with bare UV-100 (Table 1, entries 7-11). On the other hand, UV-100 samples with 0.1 wt% photodeposited noble metal (Pd, Ru, and Rh) shows significantly lower conversion of the probe compound (60%, 49%, and 30%, respectively) than UV-100 even though the selectivity remained high (97%, 100%, and 88%) (Table 1, entries 12-14). The specific surface area of UV-100 and surface grafted TiO_2 with nickel ions was measured to be 320 m^2/g and 318 m^2/g, respectively while showing similar nitrogen physisorption isotherms (SI Figure S8). No peaks corresponding to metallic nickel or nickel oxide were observed on X-ray diffractograms (SI, Figure S2) while TEM micrographs show a highly porous morphology with a particle size of 3-5 nm (SI, Figure S3).

The time-dependent experiments were performed with the optimized reaction condition using *i*-PrOH as a solvent and UV-100 in the presence or the absence of 4-amino TEMPO, and 0.1 wt% Ni(II) grafted UV-100 in the presence of 4-amino-TEMPO as photocatalysts under visible light illumination. The formations of the yield and the selectivity of the dehydrogenation reaction of 1,2,3,4-THQ in the presence of three different photocatalysts within 24 hours with 3 hours time interval have been calculated from GC-FID data (Equation 1 and 3) and are shown in **Figure 3**. As becomes obvious from **Figure 3 (a),** large amounts of quinoline are produced in the presence of Ni (II)-grafted UV-100 and 4-amino TEMPO. Significantly lower amounts of product were obtained in the presence as well as in the absence of 4-amino-TEMPO. Accordingly, the yields at a point in time during illumination calculated from the data given in **Figure 3 (a)** were found to decrease in the order Ni(II)/UV-100 + 4-amino-TEMPO > UV-100 + 4-amino-TEMPO > UV-100 **(Figure 3b)**. The results reveal that 4-amino-TEMPO significantly improves the reaction

selectivity. Concomitantly, the selectivity was observed to be ~10 % higher when Ni(II)-grafted UV-100 is used instead of suspension containing bare UV-100.

Using the improved photocatalyst, 0.1 wt% Ni(II) ion-grafted TiO_2, we compared TEMPO and three other TEMPO derivatives in the dehydrogenation reaction, establishing 4-amino-TEMPO as the optimal redox mediator for improving selectivity (Table 1, entries 15-18).

The range of substrates was investigated under the optimized reaction conditions inspired by the high photocatalyst activity of 0.1 wt% Ni/UV-100 and 20 mol% 4-amino-TEMPO in *i*-PrOH and an O_2 atmosphere (1 atm) at room temperature (Table 2). 1,2,3,4-THQs bearing a methoxy **(2b)**, methyl **(2c** and **2f)**, chloride **(2e),** or both a methyl and carboxyl group **(2g)** gave good to excellent yields of quinolines. However, 1,2,3,4-THQs having a nitro or a hydroxy group at C-7 failed to dehydrogenate. The inactivity of the former substrate was probably due to difficult oxidation of the aniline moiety caused by the strongly electron-withdrawing nitro group. Whereas the inertness of the hydroxylated compound is probable owning to a competitive complex formation on the TiO_2 surface via the hydroxyl group. To test this hypothesis, the OH group was protected as TBDMS (tert-butyldimethylsilyl) ether and then subjected to the standard conditions. The desired quinoline **2d** was isolated in 83% yield. 1,2,3,4-Tetrahydroisoquinolines reacted quite differently from other *N*-heterocycles as they easily afford the partial dehydrogenation product under the reaction conditions optimized for the dehydrogenation of tetrahydroquinolines. The unsubstituted tetrahydroisoquinoline gave a mixture of the completely dehydrogenated product **2h** and the partially dehydrogenated product **2h*** in 42% yield and 52% yield, respectively. Raising the reaction temperature to 47 °C improved the conversion to the completely dehydrogenated product, and the fully aromatized product **2i** was obtained in 75% yield. However, when the methyl substituent of 1-methyl-1,2,3,4-tetrahydroisoquinoline is

replaced by a larger group such as phenyl, the partially dehydrogenated product **2k*** was found to be the major product 54% yield with only 33% of the completely dehydrogenated product **2k** even when the temperature is raised to 47°C. Interestingly, 6,7-dimethoxy-1,2,3,4-tetrahydroisoquinoline only yields the completely dehydrogenated product **2j** in 81% yield at room temperature. The enhanced reactivity of this compound is presumably due to the presence of the two electron-donating methoxy groups.

The developed method was also applied to the dehydrogenation of indoline and 2-methylindoline under the optimized reaction condition with slight changes. Thus, the O_2 amount in air was found to be sufficient to mediate the dehydrogenation of unsubstituted indoline to indole **2n** in 84% yield. Significant decomposition of the reactant was observed when the reaction was performed in an O_2 atmosphere (1 atm) thus revealing that indoline is more reactive than the 1,2,3,4-tetrahydroquinolines. On the other hand, 2-methyl-substituted indoline was shown to be less reactive and more tolerant towards O_2 than unsubstituted indoline. An O_2 pressure of 1 atm was required to produce 2-methylindole **2o** in good yield (76%). 1,2,3,4-tetrahydroquinoxaline, which was also exhibited good reactivity, yielded quinoxaline **2l** in 83% yield using 1 atm O_2. Similar to indolines and quinolines, dehydrogenation of 2-phenyl-2-imidazoline to 2-phenylimidazole **2m** was achieved with an excellent reaction efficiency (93%) under optimized reaction condition.

Since the leaching of the impregnated active metal ion sites during the reaction, phase transformation, and agglomeration of nanoparticles is ubiquitous in heterogeneous photocatalysis, we examined the reusability of 0.1 wt% Ni/TiO_2 by performing four consecutive experimental runs (See SI for details on the recycling procedure). Conversion of the probe compound, as well as the yield of the product and the selectivity of product formation, was found

to be stable even after 4 cycles **(Figure 4)**. The surface area of the photocatalyst decreased from 318 m^2/g to 217 m^2/g after the 2nd cycle of the reaction but remained relatively constant after the 3rd and 4th cycles (210 and 206 m^2/g, respectively). However, the surface area was restored from 206 m^2/g after the 4th cycle to 313 m^2/g by dispersing the used photocatalyst in 20 mL deionized water and illuminating with a 500 W solar simulator lamp for 2 hours at ambient temperature. The photocatalyst's color also turned from pale yellow to pure white during illumination and the surface-cleaned catalyst displayed high reactivity (91% yield) and selectivity (93%) in the 5th cycle **(Figure 4)**. N_2 adsorption-desorption isotherm studies show that although the catalyst's mesoporosity decreases after the 4th cycle, the selectivity does not decrease drastically. Additionally, cleaning the catalyst's surface by illumination led to recovering the pore size that showed adsorption-desorption isotherm similar to non-used 0.1 wt% Ni/TiO_2 (SI Figure S8).

XRD and ICP-OES measurements did not reveal poisoning and leaching of the photocatalyst, respectively. XRD patterns for bare TiO_2, 0.1 wt% Ni/UV-100 before the 1st cycle and after the 4th cycle displayed the typical crystal structure of the anatase phase without showing the peaks corresponding to the nickel ion (SI Figure S2). Moreover, the ICP-OES measurement showed that the content of nickel ions before and after the reaction did not change drastically (before and after 4th cycle of reaction the content of nickel was 0.08 wt% with respect to TiO_2; see SI for sample preparation for the ICP-OES measurement).

ATR-FTIR spectroscopy measurements were conducted to detect functional groups of organic compounds adsorbed on the catalyst's surface after the dehydrogenation reaction. Characteristic bands at 2950 cm^{-1}, 2370 cm^{-1}, and 1640 cm^{-1}, which were assigned to the stretching of C-H, C-O and O-H groups of *i*-PrOH, respectively, as well as the broad band at 3400 cm^{-1}, which corresponds to the OH stretching of surface-adsorbed water molecules, were observed in all

spectra (**Figure 5**). The intensity of this broad band at 3400 cm^{-1}, was observed to start to decrease after the 3rd cycle. The decline of the intensity of the OH stretching band was rationalized by a gradual accumulation of organic compounds at the catalyst's surface that results in a displacement of the surface-adsorbed water by organic compounds. On the other hand, the band at 1681cm^{-1}, which was attributed to the C=N stretching, was observed only after the 3rd cycle and disappeared after the catalyst was subjected to surface cleaning by solar light illumination. Characteristic peaks of aromatic rings in the range of 1561 cm^{-1} (C=C), 1429 cm^{-1} (C-C), and 1276 cm^{-1} (Ar-N), were detected only in the used 0.1 wt% Ni/TiO_2. This observation was expected as those peaks were assigned to the imine products that were bound to the Lewis acidic TiO_2 surface.[42] Based on the obtained results we propose a tentative mechanism for the dehydrogenation reaction of tetrahydroquinolines as illustrated in **Scheme 2.**

The 1,2,3,4-THQs binds to the surface of UV-100 to form a surface complex, which absorbs visible light to become excited. Subsequently, the excited tetrahydroquinoline injects an electron into the conduction band of the semiconductor UV-100. After being temporarily stored on the surface grafted Ni ion, the photogenerated electron reduces O_2 yielding the superoxide radical anion. This radical anion abstracts two protons and one electron from the tetrahydroquinoline radical cation thus forming the C=N bond. This sequence of reaction steps is repeated with the partially dehydrogenated product as the reactant to complete the aromatization to the quinoline. The grafted Ni ion ($E°(Ni^{2+}/Ni^{0})$= -0.26V vs. NHE) [43] likely plays the role of an electron shuttle which not only hinders the fast decay of the photogenerated electrons but also promotes the reduction of O_2 by conduction band electrons, thus enhancing the overall photo-activity of UV-100. However, noble metal co-catalysts demonstrate relatively low reaction yield which can be

explained by their electron scavenging capacity that retards the reaction momentum, eventually causing low activity.

In situ EPR measurements were performed with powders of 0.1 wt% Ni/UV-100 and bare TiO_2 (UV-100) at 77 K in an argon atmosphere to examine the impact of the grafted Ni ion on the electron shuttle process (**Figure 6**). In the dark, both samples showed characteristic peaks with g values of g_1=2.027, g_2=2.009 and g_3=2.005 (Signals D) which has been assigned to Ti^{4+}-$O_2^{-\bullet}$ species.[44] Upon UV-vis illumination, peaks at g_1=2.018, g_2=2.014 and g_3=2.005 (Signals A) were generated which have been proposed to correspond to the trapped holes, i.e., Ti^{4+}-$O^{\cdot-}$-Ti^{4+}-OH^- radicals at the surface sites of TiO_2. [45,46] Additionally, signals $g_{\parallel}$=1.96 and $g_{\perp}$=1.990 (Signals B) are formed during irradiation. These signals are indicating the presence of Ti^{3+} which are formed by trapping of photogenerated electrons.[47] The intensity of the signals B of the Ni/UV-100 photocatalyst is drastically decreased in comparison with bare TiO_2 **(Figure 6 (a))**. This observation is consistent with a previous report [48], which proved that the grafted Ni(II) ions located on the surface and surface defects of TiO_2, reduce the amount of Ti^{3+} species by trapping photogenerated electrons. The broad weak signal at around g = 2.06 (Signal C) observed in both bare TiO_2 and 0.1 wt% Ni/UV-100 corresponds to the surface-adsorbed O_2 molecules, which act as an electron acceptors. [49]

The presence of a redox mediator such as TEMPO and 4-amino-TEMPO in the photocatalyst suspension was found to have only a small impact on the conversion of the reactant but it significantly increased the yield and selectivity of the desired reaction product (Table 1, entry 1-3). The substantial effect shown by 4-amino-TEMPO prompted us to investigate its role in the dehydrogenation reaction. To the best of our knowledge, TEMPO has been reported only by Zhao[50] and Chen[51] as a cocatalyst in TiO_2-catalyzed photochemistry. Somewhat related to this

method, Lei reported the use of TEMPO as an organo-electrocatalyst in electrochemical dehydrogenation of *N*-heterocycles in N_2 atmosphere where TEMPO was proposed to be directly responsible for the oxidation of *N*-heterocycles and subsequent dehydrogenation.[52] However, we observed that 4-amino-TEMPO plays a different role in this method. Our hypothesis is built upon a noticeable phenomenon we observed during the screen studies. Without any redox mediator namely 4-amino-TEMPO in the suspension (Table 1, entry 1) the initially light yellow suspension became dark brown during the light-induced reaction in addition to the accompanied low selectivity and yield. In contrast, in the presence of 4-amino-TEMPO, the reaction color maintained light yellow throughout the reaction. We attribute the low conversion and selectivity and the color change observed in the absence of 4-amino-TEMPO to the formation of H_2O_2/TiO_2 surface complexes (See SI Figure S7), which saturate the TiO_2 surface and prevent the formation of the N-heterocycle-TiO_2 surface complex necessary for an efficient electron transfer from the excited organic moiety to the conduction band of the semiconducting TiO_2. TEMPO and its derivatives are known to be stable radicals and bear one-electron reversible oxidation to form oxoammonium salts ($TEMPO^+$).[53] These compounds have been investigated as redox mediators for electrochemically oxidizing primary and secondary alcohols.[54,55] Sen and his group have introduced the oxidation of hydrogen peroxide molecules over 4-hydroxy TEMPO.[56] Lately, it has been reported the electrocatalytic anodic oxidation of H_2O_2 by nitroxyl radicals and revealed that among the TEMPO series, 4-amino-TEMPO shows the highest catalytic efficiency due to the strong electron-withdrawing effect of an amino substituent.[57] This evidence is in agreement with our observation. Taking into account of developed insights over nitroxyl radicals, we have anticipated the ongoing reaction pathways in our system. (Eqs. (5)-(8)).

$$H_2O_2 + Ti^{IV}_{(surf.)} \rightleftharpoons Ti^{IV} - OOH_{(surf.)} + H^+ \quad (5)$$

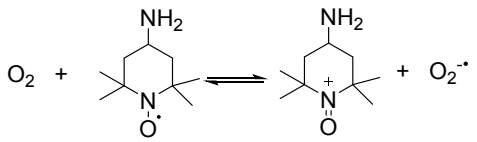

(6)

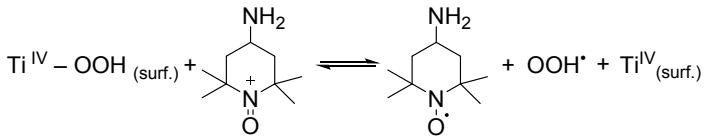

(7)

(8)

Thus, the generation of hydrogen peroxide molecules as a byproduct during the dehydrogenation process of N-heterocycles initiates the formation of a surface complex with titania (Eq. (5). Since 4-amino-TEMPO shows weak absorption at the visible light region of 470 nm (SI Figure S6) we expected the oxidation of TEMPO to the $TEMPO^+$ and one-electron reduction of an oxygen molecule to the superoxide radical anion (Eq. (6)). On the other hand, in contrast to TEMPO, $TEMPO^+$ is not paramagnetic. Therefore, to support this suggestion, EPR experiments with 4-amino-TEMPO in the presence and in the absence of visible light (λ= 453 nm) illumination in an oxygen atmosphere have been performed. The results show that the intensity of the EPR signals belonging to 4-amino-TEMPO slightly decreases upon illumination which is suggesting that the cation 4-amino-$TEMPO^+$ is formed upon visible light illumination (SI Figure S10). Hence, the generated oxoammonium cation leads to the decomposition of the surface titanium (IV) hydrogen peroxide complex and subsequent generation of a superoxide radical (Eqs. (7)-(8)).

To test this hypothesis, we measured the concentration of H_2O_2 formed during the dehydrogenation reaction in the absence (Table 1, entry 1) and the presence of 4-amino-TEMPO (Table 1, entry 2). Indeed, the concentration of H_2O_2 is observed to be significantly higher in the

absence of 4-amino-TEMPO (see SI Figure S11).[25] The lower concentration of H_2O_2, which is a strong oxidizing agent, observed in the presence of the 4-amino-TEMPO resulted in minimizing possible side reactions, thus improving the selectivity of the desired reaction.

Conclusions

In summary, a visible-light-mediated aerobic dehydrogenation method of N-heterocyclic amines is developed using commercially available anatase TiO_2, UV-100. By employing three-pronged approach (visible light excitation of a N-heterocycle-TiO_2 surface complex, Ni(II) ion-grafted TiO_2, and 4-amino-TEMPO for improving selectivity) we successfully achieved to activate the UV-active TiO_2 to be a highly selective visible light responsive photocatalyst. The conspicuous studies regarding the N-heterocycle/TiO_2 surface complex formation supported that organic transformation over bare TiO_2 upon visible light illumination is practicable. The essential role of 4-amino-TEMPO was improving reaction selectivity to prevent the saturation of the TiO_2 surface by H_2O_2 and also assist its degradation. The surface-grafted TiO_2 with 0.1 wt% Ni(II) ion improved the yield and the selectivity, most probably because the metal ion acts as an electron transfer bridge, and reduction process occurs to produce superoxide radical anions. One of the well-known issues that plague TiO_2 as a successful photocatalyst in organic synthesis is non-selective oxidation of organic reactants and products resulting in poor yields and selectivity. The present approach employing TiO_2 as the photocatalyst and 4-amino-TEMPO as a selective redox mediator under mild reaction conditions effectively overcomes this existing issue for synthesizing N-heterocyclic aromatic compounds. Importantly, the present method comprises low-cost, environmentally friendly photocatalyst, and visible light. Moreover, the photocatalytic system maintains its chemical stability presenting high selectivity and the reaction yield over

recycles. The achieved results demonstrate that the method is remarkably applicable for the numerous substrate scopes.

FIGURES

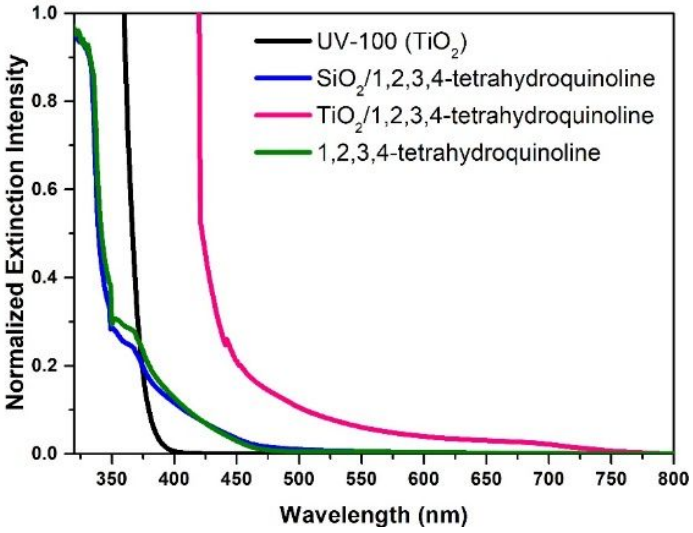

Figure 1. Normalized extinction spectra for the bare TiO_2 (UV-100), SiO_2/1,2,3,4-tetrahydroquinoline, TiO_2/1,2,3,4-tetrahydroquinoline, and 1,2,3,4-tetrahydroquinoline. Absorption spectroscopy measurements were performed at the same concentration of the catalyst and substrate as appropriate to the organic reaction condition in a CH_3CN solvent.

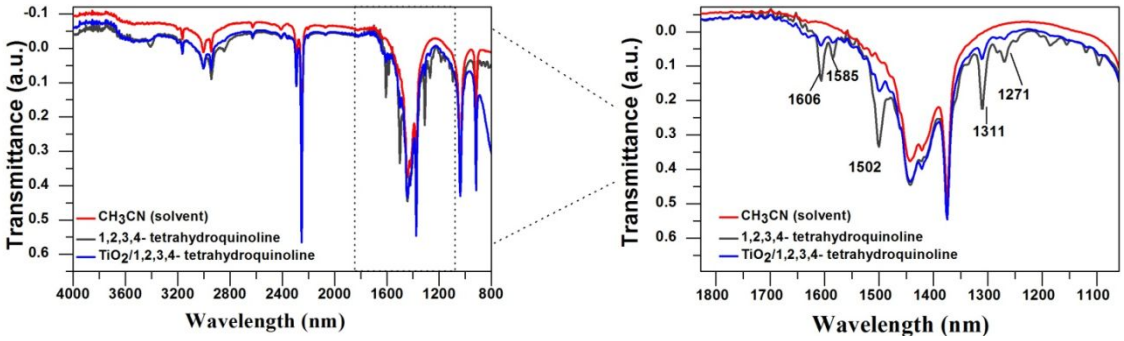

Figure 2. FTIR spectra of CH_3CN solvent, 1,2,3,4-tetrahydroquinoline, and UV-100 (TiO_2) / 1,2,3,4-tetrahydroquinoline suspension. The right figure shows magnification of the area

between dashed lines in the left figure. All measurements were performed at the same concentration of the catalyst and substrate as appropriate to the organic reaction condition.

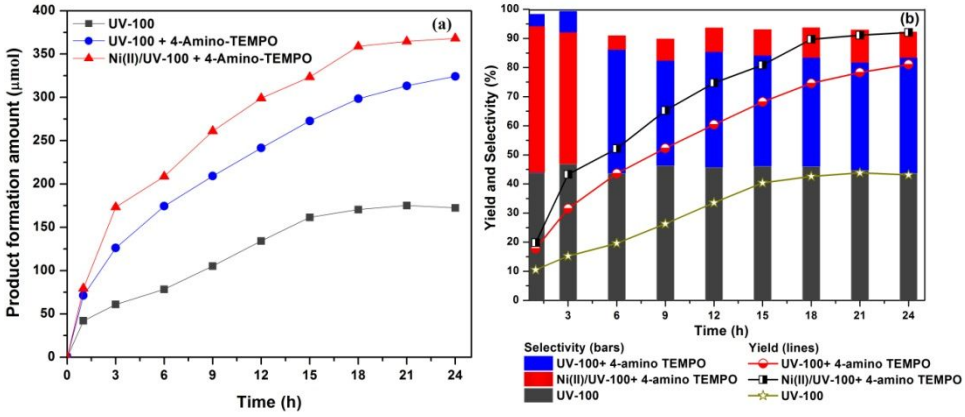

Figure 3. Amounts of products formed during 24 h of illumination (a) and time-dependent change in the yield and selectivity (b). Reactions conditions: 10 mg photocatalysts (UV-100 or Ni (II)-grafted UV-100), LED lamp, λ=453nm, 4 mW/cm^2, 1 atm O_2, 0.4 mmol 1,2,3,4-THQ, 0.08 mmol 4-amino-TEMPO, 4 mL *i*-PrOH.

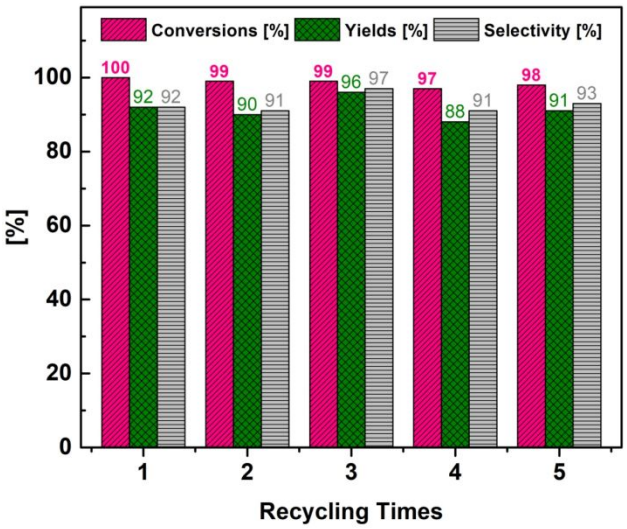

Figure 4. Oxidative dehydrogenation of 1,2,3,4-tetrahydroquinoline: recycling of 0.1 wt% Ni/TiO_2. Reactions condition: 10 mg photocatalyst, 24 hours visible light illumination (LED

lamp, λ=453nm, 4 mW/cm^2), 1 atm O_2, 0.4 mmol 1,2,3,4-THQ, 0.08 mmol 4-amino-TEMPO, 4 mL *i*-PrOH. The 5th cycling was performed after cleaning the catalyst by solar light illumination for 2 h. Yields calculated according to the GC-FID calibration using benzyl alcohol as an internal standard.

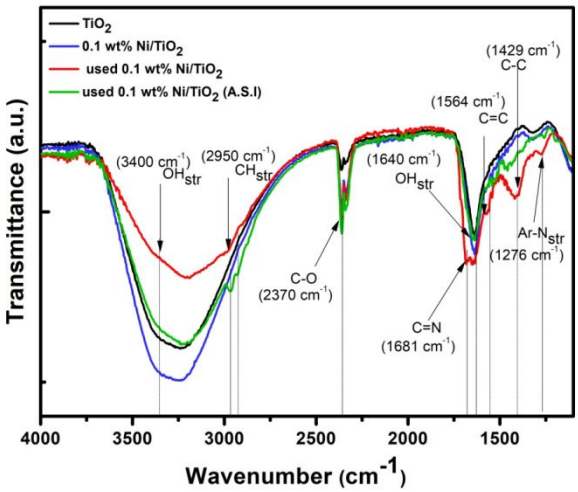

Figure 5. ATR-FTIR spectra of the bare TiO_2 (UV-100) (black line), 0.1 wt% Ni grafted TiO_2 before reaction (blue line), used 0.1 wt% Ni grafted TiO_2 after 3 cycles of the reaction (red line), and used 0.1 wt% Ni grafted TiO_2 after cleaning with 500W solar simulator light (green line)

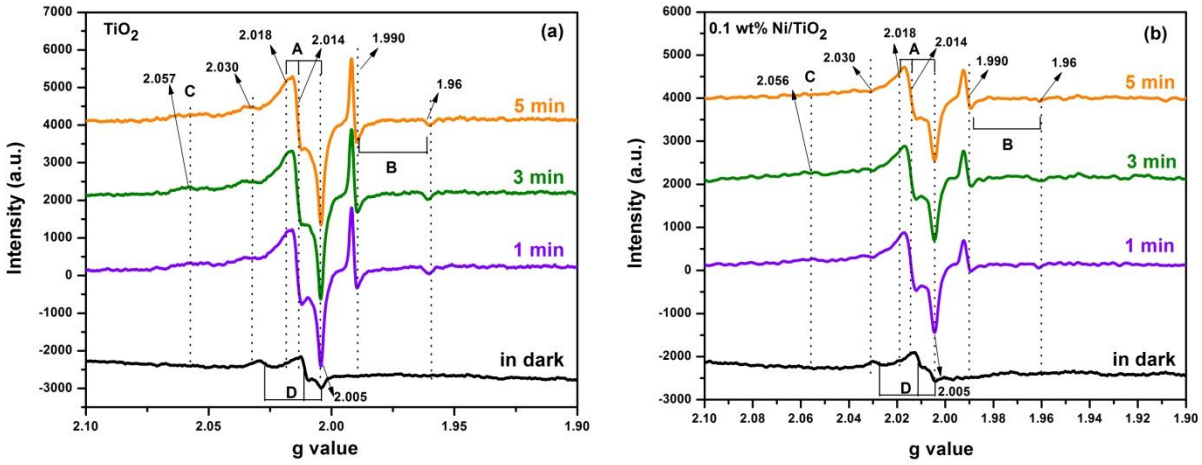

Figure 6. In situ EPR spectra at 77K of TiO_2 (a) and 0.1 wt% Ni(II) ion-grafted TiO_2 (b) in the dark and under 1 min; 2 min; 3 min; and 5 min UV-vis light irradiation (Xe lamp, λ=300-450nm). The spectra under light irradiation are obtained by subtracting the spectrum in the dark.

SCHEMES

Previous works:

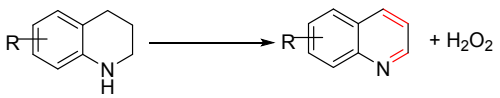

1) $Ru(bpy)_3^{2+}$, visible light, O_2, r.t.

2) Organo-photoredox, air, visible light, r.t.

This work:

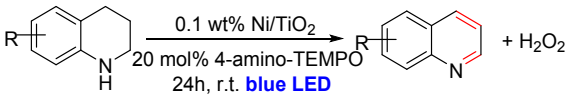

- ✓ **Non-toxic photocatalysts/solvent**
- ✓ **Low-cost**
- ✓ **Recyclable/reuse**
- ✓ **Noble metal free**

Scheme 1. Oxidative dehydrogenation of N-heterocyclic amines into the corresponding imines.

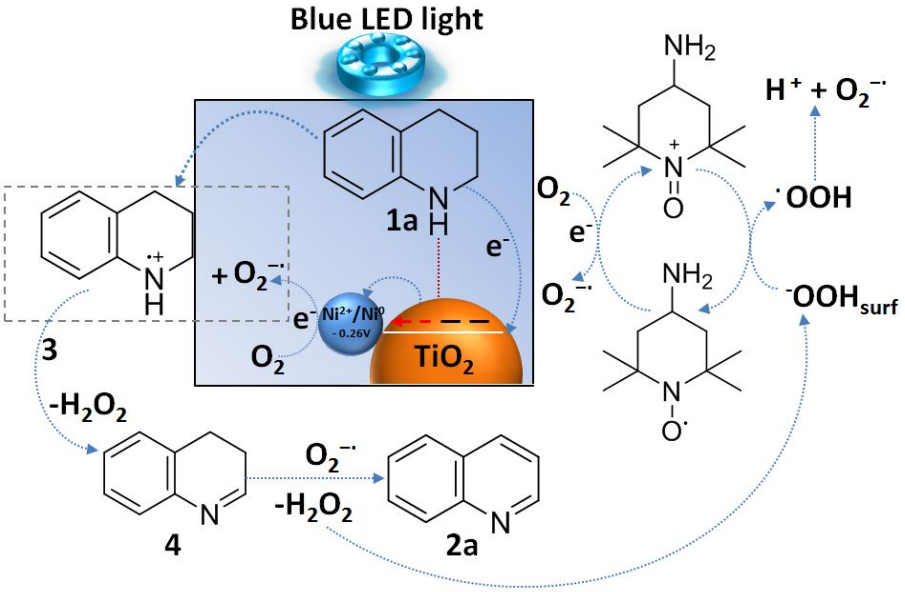

Scheme 2. A plausible mechanism of the ongoing reaction in the presence of 4-amino-TEMPO and surface-grafted 0.1 wt% Ni/TiO_2 photocatalyst.

Table 1. Optimization of the reaction conditions [a]

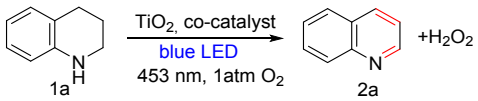

Entry	Catalysts	Redox mediator	C (%)	Y (%) [b]	S (%) [c]	Φ_{App}
1[d]	UV-100	-	81	35	43	$0.95\cdot10^{-2}$
2	UV-100	4-amino-TEMPO	98	79	81	$2.14\cdot10^{-2}$
3	UV-100	TEMPO	86	70	81	$1.90\cdot10^{-2}$
4	P25	-	24	10	42	$0.27\cdot10^{-2}$
5[e]	-	4-amino-TEMPO	3	3	100	$0.08\cdot10^{-2}$
6[d]	UV-100 (in dark)	-	n.d.	n.d.	n.d.	-
7	Cu/UV-100	4-amino-TEMPO	100	91	91	$2.47\cdot10^{-2}$
8	Ni/UV-100	4-amino-TEMPO	100	91	91	$2.47\cdot10^{-2}$
9	Nb/UV-100	4-amino-TEMPO	95	90	95	$2.44\cdot10^{-2}$
10	Fe/UV-100	4-amino-TEMPO	100	90	90	$2.44\cdot10^{-2}$
11	Co/UV-100	4-amino-TEMPO	100	93	93	$2.52\cdot10^{-2}$
12	Pd/UV-100	4-amino-TEMPO	62	60	97	$1.63\cdot10^{-2}$
13	Ru/UV-100	4-amino-TEMPO	49	49	100	$1.33\cdot10^{-2}$
14	Rh/UV-100	4-amino-TEMPO	34	30	88	$0.81\cdot10^{-2}$
15[f]	Ni/UV-100	TEMPO	80	58	73	$1.57\cdot10^{-2}$
16[f]	Ni/UV-100	4-hydroxy-TEMPO	69	58	88	$1.57\cdot10^{-2}$
17[f]	Ni/UV-100	4-oxo-TEMPO	93	77	83	$2.09\cdot10^{-2}$
18[f]	Ni/UV-100	4-amino-TEMPO	100	92(91[g])	92	$2.49\cdot10^{-2}$
19	Ni/UV-100	-	93	57	61	$1.54\cdot10^{-2}$

[a] Reactions condition: 10 mg photocatalyst TiO_2 (UV-100 or P25), 24 h visible light illumination (LED lamp, λ=453nm, 4 mW/cm^2), 1 atm O_2, 0.4 mmol 1,2,3,4-THQ, 0.08 mmol TEMPO derivatives, 4 mL CH_3CN. [b] calculated according to the GC-FID calibration using benzyl alcohol as an internal standard. [c] ratio of yield over conversion. [d] no TEMPO. [e] no TiO_2. [f] *i*-PrOH instead of CH_3CN. [g] isolated yield.

Table 2. Dehydrogenation of other derivatives of N-heterocyclic amines [a]

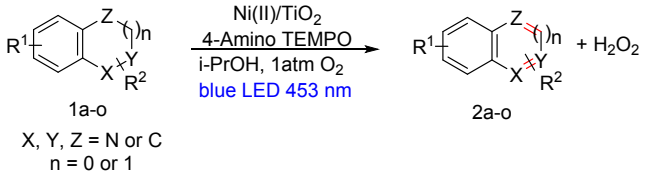

Entry	Substrates	Products	Yield (%)[b]
1	1a	2a	91
2	1b	2b	94
3	1c	2c	91
4	1d	2d	83
5	1e	2e	92
6	1f	2f	74
7	1g	2g	93
8	1h	2h, 2h*	42; 52*
9[c]	1i	2i	75
10[d]	1j	2j	81
11[c]	1k	2k, 2k*	33; 54*
12	1l	2l	83
13	1m	2m	93
14[e]	1n	2n	84
15	1o	2o	76

[a] Reactions condition: 10 mg photocatalyst, 24 hours visible light illumination (LED lamp, λ=453 nm, 4 mW/cm^2), 1 atm O_2, 0.4 mmol organic substrate, 0.08 mmol 4-amino-TEMPO, 4 mL *i*-PrOH, room temperature. [b] The yields are those of the isolated products. [c] 47 °C. [d] 1:1 CH_2Cl_2: *i*-PrOH was used as the solvent. [e] Air was used. * Partial dehydrogenation yield.

ASSOCIATED CONTENT

Supporting information. A listing of the contents of each file supplied as SI should be included. For instructions on what should be included in the SI as well as how to prepare this material for publications, refer to the journal's Instructions for Authors.

The following files are available free of charge.

Materials and chemicals, results of the analytical methods (GC-FID, XRD, TEM, UV-vis, BET, ICP-OES, EPR, ATR-FTIR, and FTIR), data of control reactions, catalyst recycling procedure, detection of hydrogen peroxide, NMR characterization of compounds (PDF).

AUTHOR INFORMATION

Corresponding Author

*Narmina O. Balayeva; balayeva@iftc.uni-hannover.de

* Nan Zheng; nzheng@uark.edu

* Detlef W. Bahnemann; bahnemann@iftc.uni-hannover.de

Author Contributions

The manuscript was written through contributions of all authors. All authors have given approval to the final version of the manuscript.

ACKNOWLEDGMENT

Narmina Balayeva gratefully acknowledges the financial support from Graduate Academy of Leibniz University Hannover in the frame of "Research Stay Abroad Program" at the University

of Arkansas, Chemistry and Biochemistry Department. The authors would like to thank M.Sc. Barbara Nunes from Prof. D. Bahnemann group, Institute of Technical Chemistry at the Leibniz University of Hannover for XRD and TEM measurement, and M.Sc. Malte Schäfer from Prof. P. Behrens group, Institute of Inorganic Chemistry at the Leibniz University of Hannover for the BET (physisorption isotherms) measurement. Institute of Geology for ICP-OES, Laboratorium für Nano- und Quantenengineering (LNQE) for TEM and Institute of Inorganic Chemistry at the Leibniz University of Hannover for ATR-FTIR and BET equipment are kindly acknowledged.

REFERENCES

(1) Dobereiner, G. E.; Crabtree, R. H. Dehydrogenation as a Substrate-Activating Strategy in Homogeneous Transition-Metal Catalysis. *Chem. Rev.* **2010**, *110*, 681–703.

(2) Choi, J.; MacArthur, A. H. R.; Brookhart, M.; Goldman, A. S. Dehydrogenation and Related Reactions Catalyzed by Iridium Pincer Complexes. *Chem. Rev.* **2011**, *111*, 1761–1779.

(3) Yamaguchi, R.; Ikeda, C.; Takahashi, Y.; Fujita, K. I. Homogeneous Catalytic System for Reversible Dehydrogenation-Hydrogenation Reactions of Nitrogen Heterocycles with Reversible Interconversion of Catalytic Species. *J. Am. Chem. Soc.* **2009**, *131*, 8410–8412.

(4) Wang, Z.; Tonks, I.; Belli, J.; Jensen, C. M. Dehydrogenation of N-Ethyl Perhydrocarbazole Catalyzed by PCP Pincer Iridium Complexes: Evaluation of a Homogenous Hydrogen Storage System. *J. Organomet. Chem.* **2009**, *694*, 2854–2857.

(5) Muthaiah, S.; Hong, S. H. Acceptorless and Base-Free Dehydrogenation of Alcohols and Amines Using Ruthenium-Hydride Complexes. *Adv. Synth. Catal.* **2012**, *354*, 3045–3053.

(6) Luca, O. R.; Huang, D. L.; Takase, M. K.; Crabtree, R. H. Redox-Active

Cyclopentadienyl Ni Complexes with Quinoid N-Heterocyclic Carbene Ligands for the Electrocatalytic Hydrogen Release from Chemical Fuels. *New J. Chem.* **2013**, *37*, 3402–3405.

(7) Xu, R.; Chakraborty, S.; Yuan, H.; Jones, W. D. Acceptorless, Reversible Dehydrogenation and Hydrogenation of *N* -Heterocycles with a Cobalt Pincer Catalyst. *ACS Catal.* **2015**, *5*, 6350–6354.

(8) Fu, P. P.; Harvey, R. G. Dehydrogenation of Polycyclic Hydroaromatic Compounds. *Chem. Rev.* **1978**, *78*, 317–361.

(9) Hara, T.; Mori, K.; Mizugaki, T.; Ebitani, K.; Kaneda, K. Highly Efficient Dehydrogenation of Indolines to Indoles Using Hydroxyapatite-Bound Pd Catalyst. *Tetrahedron Lett.* **2003**, *44*, 6207–6210.

(10) Moromi, S. K.; Siddiki, S. M. A. H.; Kon, K.; Toyao, T.; Shimizu, K. Acceptorless Dehydrogenation of N -Heterocycles by Supported Pt Catalysts. *Catal. Today* **2017**, *281*, 507–511.

(11) Ainembabazi, D.; An, N.; Manayil, J. C.; Wilson, K.; Lee, A. F.; Voutchkova-Kostal, A. M. Acceptorless Amine Dehydrogenation and Transamination Using Pd-Doped Hydrotalcites. *ACS Catal.* **2019**, *9*, 1055–1065.

(12) Oyama, T.; Yatabe, T.; Jin, X.; Mizuno, N.; Yamaguchi, K. Heterogeneously Palladium-Catalyzed Acceptorless Dehydrogenative Aromatization of Cyclic Amines. *Chem. Lett.* **2019**, *48* , 517–520.

(13) Walker, D.; Hiebert, J. D. 2,3-Dichloro-5,6-Dicyanobenzoquinone and Its Reactions. *Chem. Rev.* **1967**, *67*, 153–195.

(14) Kitamura, M.; Yoshida, M.; Kikuchi, T.; Narasaka, K. Synthesis of Quinolines and 2H-

Dihydropyrroles by Nucleophilic Substitution at the Nitrogen Atom of Oxime Derivatives. *Synthesis (Stuttg)*. **2003**, *2003*, 2415-2426.

(15) Jung, D.; Kim, M. H.; Kim, J. Cu-Catalyzed Aerobic Oxidation of Di- *Tert* -Butyl Hydrazodicarboxylate to Di- *Tert* -Butyl Azodicarboxylate and Its Application on Dehydrogenation of 1,2,3,4-Tetrahydroquinolines under Mild Conditions. *Org. Lett.* **2016**, *18,* 6300-6303.

(16) Shang, Y.; Jie, X.; Jonnada, K.; Zafar, S. N.; Su, W. Dehydrogenative Desaturation-Relay via Formation of Multicenter-Stabilized Radical Intermediates. *Nat. Commun.* **2017**, *8*, 2273.

(17) Zumbrägel, N.; Sako, M.; Takizawa, S.; Sasai, H.; Gröger, H. Vanadium-Catalyzed Dehydrogenation of *N* -Heterocycles in Water. *Org. Lett.* **2018**, *20*, 4723–4727.

(18) Li, J.; Liu, G.; Long, X.; Gao, G.; Wu, J.; Li, F. Different Active Sites in a Bifunctional Co@N-Doped Graphene Shells Based Catalyst for the Oxidative Dehydrogenation and Hydrogenation Reactions. *J. Catal.* **2017**, *355*, 53-62.

(19) Iosub, A. V.; Stahl, S. S. Catalytic Aerobic Dehydrogenation of Nitrogen Heterocycles Using Heterogeneous Cobalt Oxide Supported on Nitrogen-Doped Carbon. *Org. Lett.* **2015**, *17*, 4404-4407.

(20) So, M.-H.; Liu, Y.; Ho, C.-M.; Che, C.-M. Graphite-Supported Gold Nanoparticles as Efficient Catalyst for Aerobic Oxidation of Benzylic Amines to Imines and *N* -Substituted 1,2,3,4-Tetrahydroisoquinolines to Amides: Synthetic Applications and Mechanistic Study. *Chem. - An Asian J.* **2009**, *4* , 1551–1561.

(21) Jawale, D. V.; Gravel, E.; Shah, N.; Dauvois, V.; Li, H.; Namboothiri, I. N. N.; Doris, E. Cooperative Dehydrogenation of N-Heterocycles Using a Carbon Nanotube-Rhodium

Nanohybrid. *Chem. - A Eur. J.* **2015**, *21*, 7039–7042.

(22) Kumaran, E.; Leong, W. K. Gold(0) Catalyzed Dehydrogenation of N-Heterocycles. *Tetrahedron Lett.* **2018**, *59*, 3958–3960.

(23) Chen, S.; Wan, Q.; Badu-Tawiah, A. K. Picomole-Scale Real-Time Photoreaction Screening: Discovery of the Visible-Light-Promoted Dehydrogenation of Tetrahydroquinolines under Ambient Conditions. *Angew. Chemie - Int. Ed.* **2016,** *55*,9345–9349.

(24) Kojima, M.; Kanai, M. Tris(Pentafluorophenyl)Borane-Catalyzed Acceptorless Dehydrogenation of N-Heterocycles. *Angew. Chemie - Int. Ed.* **2016**, *55*, 12224–12227.

(25) Sahoo, M. K.; Jaiswal, G.; Rana, J.; Balaraman, E. Organo-Photoredox Catalyzed Oxidative Dehydrogenation of N-Heterocycles. *Chem. - A Eur. J.* **2017,** *23*, 14167–14172.

(26) He, K.-H.; Tan, F.-F.; Zhou, C.-Z.; Zhou, G.-J.; Yang, X.-L.; Li, Y. Acceptorless Dehydrogenation of N-Heterocycles by Merging Visible-Light Photoredox Catalysis and Cobalt Catalysis. *Angew. Chemie Int. Ed.* **2017**, *56*, 3080–3084.

(27) Friedmann, D.; Hakki, A.; Kim, H.; Choi, W.; Bahnemann, D. Heterogeneous Photocatalytic Organic Synthesis: State-of-the-Art and Future Perspectives. *Green Chem.* **2016**, *18*, 5391-5411.

(28) Balayeva, N. O.; Fleisch, M.; Bahnemann, D. W. Surface-Grafted WO3/TiO2 Photocatalysts: Enhanced Visible-Light Activity towards Indoor Air Purification. *Catal. Today* **2018**, *313*, 63–71.

(29) Pelaez, M.; Nolan, N. T.; Pillai, S. C.; Seery, M. K.; Falaras, P.; Kontos, A. G.; Dunlop, P. S. M.; Hamilton, J. W. J.; Byrne, J. A.; O'Shea, K.; Entezari, M. H.; Dionysiou D. D. A Review on the Visible Light Active Titanium Dioxide Photocatalysts for Environmental

Applications. *Appl. Catal. B Environ.* **2012**, *125*, 331–349.

(30) Lang, X.; Ma, W.; Zhao, Y.; Chen, C.; Ji, H.; Zhao, J. Visible-Light-Induced Selective Photocatalytic Aerobic Oxidation of Amines into Imines on TiO 2. *Chem. - A Eur. J.* **2012,** *18*, 2624 – 2631.

(31) Zhang, G.; Kim, G.; Choi, W. Visible Light Driven Photocatalysis Mediated via Ligand-to-Metal Charge Transfer (LMCT): An Alternative Approach to Solar Activation of Titania. *Energy Environ. Sci.* **2014**, *7*, 954-966.

(32) Kumar, S. G.; Devi, L. G. Review on Modified TiO2 Photocatalysis under UV/Visible Light: Selected Results and Related Mechanisms on Interfacial Charge Carrier Transfer Dynamics. *J. Phys. Chem. A* **2011**, *115*, 13211–13241.

(33) Lang, X.; Ji, H.; Chen, C.; Ma, W.; Zhao, J. Selective Formation of Imines by Aerobic Photocatalytic Oxidation of Amines on TiO2. *Angew. Chemie - Int. Ed.* **2011**, *50*, 3934–3937.

(34) Pitre, S. P.; Yoon, T. P.; Scaiano, J. C. Titanium Dioxide Visible Light Photocatalysis: Surface Association Enables Photocatalysis with Visible Light Irradiation. *Chem. Commun.* **2017**, *53*, 4335–4338.

(35) Pitre, S. P.; Scaiano, J. C.; Yoon, T. P. Photocatalytic Indole Diels–Alder Cycloadditions Mediated by Heterogeneous Platinum-Modified Titanium Dioxide. *ACS Catal.* **2017**, *7*, 6440–6444.

(36) Shi, J.-L.; Hao, H.; Lang, X. Phenol-TiO 2 Complex Photocatalysis: Visible Light-Driven Selective Oxidation of Amines into Imines in Air. *Sustainable Energy Fuels***. 2019,** *3*, 488-498.

(37) Shi, J. L.; Hao, H.; Li, X.; Lang, X. Merging the Catechol-TiO2 Complex Photocatalyst

with TEMPO for Selective Aerobic Oxidation of Amines into Imines. *Catal. Sci. Technol.* **2018**, *8*, 3910–3917.

(38) Hao, H.; Shi, J.-L.; Xu, H.; Li, X.; Lang, X. N-Hydroxyphthalimide-TiO2 Complex Visible Light Photocatalysis. *Appl. Catal. B Environ.* **2019**, *246*, 149–155.

(39) Li, X.; Xu, H.; Shi, J. L.; Hao, H.; Yuan, H.; Lang, X. Salicylic Acid Complexed with TiO 2 for Visible Light-Driven Selective Oxidation of Amines into Imines with Air. *Appl. Catal. B Environ.* **2019**, *244*, 758–766.

(40) Irie, H.; Kamiya, K.; Shibanuma, T.; Miura, S.; Tryk, D. A.; Yokoyama, T.; Hashimoto, K. Visible Light-Sensitive Cu(II)-Grafted TiO $_2$ Photocatalysts: Activities and X-Ray Absorption Fine Structure Analyses. *J. Phys. Chem. C* **2009**, *113*, 10761–10766.

(41) Yu, H.; Irie, H.; Shimodaira, Y.; Hosogi, Y.; Kuroda, Y.; Miyauchi, M.; Hashimoto, K. An Efficient Visible-Light-Sensitive Fe(III)-Grafted TiO $_2$ Photocatalyst. *J. Phys. Chem. C* **2010**, *114* , 16481–16487.

(42) Barzetti, T.; Selli, E.; Moscotti, D.; Forni, L. Pyridine and Ammonia as Probes for FTIR Analysis of Solid Acid Catalysts. *J. Chem. Soc. Faraday Trans.* **1996**, *92*, 1401-1407.

(43) Loget, G.; Larcade, G.; Lapeyre, V.; Garrigue, P.; Warakulwit, C.; Limtrakul, J.; Delville, M. H.; Ravaine, V.; Kuhn, A. Single Point Electrodeposition of Nickel for the Dissymmetric Decoration of Carbon Tubes. *Electrochimica Acta*. **2010**, *55*, 8116-8120.

(44) C-ha, N. O. E.; Howe, R. F.; Grátzel, M. EPR Study of Hydrated Anatase under UV Irradiation. *J. Phys. Chem.* **1987**, *4*, 3906–3909.

(45) Micic, O. I.; Zhang, Y.; Cromack, K. R.; Trifunac, A. D.; Thurnauer, M. C. *Trapped Holes on T1O2 Colloids Studied by Electron Paramagnetic Resonance. J. Phys. Chem.* **1993,** *97*,7277-7283.

(46) Priebe, J. B.; Karnahl, M.; Junge, H.; Beller, M.; Hollmann, D.; Brückner, A. Angewandte Water Reduction with Visible Light : Synergy between Optical Transitions and Electron Transfer in Au-TiO 2 Catalysts Visualized by In Situ EPR Spectroscopy. *Angew. Chemie - Int. Ed.* **2013**, *52*, 11420–11424.

(47) Hirakawa, T.; Kominami, H.; Ohtani, B.; Nosaka, Y. Mechanism of Photocatalytic Production of Active Oxygens on Highly Crystalline TiO 2 Particles by Means of Chemiluminescent Probing and ESR Spectroscopy. *J. Phys. Chem.* **2001**, *105*, 6993–6999.

(48) Fan, L.; Long, J.; Gu, Q.; Huang, H.; Lin, H.; Wang, X. Single-Site Nickel-Grafted Anatase TiO2 for Hydrogen Production: Toward Understanding the Nature of Visible-Light Photocatalysis. *J. Catal.* **2014**, *320*, 147–159.

(49) Nakaoka, Y.; Nosaka, Y. ESR Investigation into the Effects of Heat Treatment and Crystal Structure on Radicals Produced over Irradiated TiO2 Powder. *J. Photochem. Photobiol. A Chem.* **1997**, *110*, 299–305.

(50) Zhang, M.; Chen, C.; Ma, W.; Zhao, J. Visible-Light-Induced Aerobic Oxidation of Alcohols in a Coupled Photocatalytic System of Dye-Sensitized TiO_2 and TEMPO. *Angew. Chemie Int. Ed.* **2008**, *47*, 9730–9733.

(51) Lang, X.; Zhao, J.; Chen, X. Visible-Light-Induced Photoredox Catalysis of Dye-Sensitized Titanium Dioxide: Selective Aerobic Oxidation of Organic Sulfides. *Angew. Chemie - Int. Ed.* **2016**, *55*, 4697–4700.

(52) Wu, Y.; Yi, H.; Lei, A. Electrochemical Acceptorless Dehydrogenation of N-Heterocycles Utilizing TEMPO as Organo-Electrocatalyst. *ACS Catal.* **2018**, *8*, 1192–1196.

(53) M. Bobbitt, J.; M. Bobbitt, J.; L. Flores, C. Prganic Nitrosonium Salts as Oxidants in Organic Chemistry. *Heterocycles.* **1988**, *27* , 509-533.

(54) Chmielewska, B.; Krzyczmonik, P.; Scholl, H. Electrode Reactions of Nitroxyl Radicals. XI: Coulometric Experiments on the Oxidation of Aliphatic Alcohols by Oxoammonium Cations. *J. Electroanal. Chem.* **1995**, *395*, 167–172.

(55) Semmelhack, M. F.; Chou, C. S.; Cortes, D. A. Nitroxyl-Mediated Electrooxidation of Alcohols to Aldehydes and Ketones. *J. Am. Chem. Soc.* **1983**, *105*, 4492–4494.

(56) Volodarsky, L. B.; Reznikov, V. A.; Ovcharenko, V. I.; Reznikov, V. A.; Ovcharenko, V. I. *Synthetic Chemistry of Stable Nitroxides*; CRC Press, **2017**.

(57) Limoges, B.; Degrand, C. Electrocatalytic Oxidation of Hydrogen Peroxide by Nitroxyl Radicals. *J. Electroanal. Chem.* **1997**, *422*, 7–12.

TOC graph